TMEM14A aggravates the progression of human ovarian cancer cells by enhancing the activity of glycolysis

QINGMEI ZHANG, XIAOHONG WANG, XUAN ZHANG, JINGFEN ZHAN, BINBIN ZHANG, JIN JIA and JIE CHEN

Department of Gynecology, The People's Hospital Affiliated to Fujian University of Traditional Chinese Medicine, Fuzhou, Fujian 350004, P.R. China

Received March 17, 2022; Accepted July 6, 2022

DOI: 10.3892/etm.2022.11551

Abstract. Ovarian cancer (OV) affects hundreds of thousands of women worldwide each year. The delayed onset of symptoms and insufficient diagnostic options of OV are mainly responsible for its high mortality rate and poor prognosis in the patients. Transmembrane (TMEM) proteins are associated with human cancers, and multiple of them have been identified as oncogenic. TMEM14A is among this group. However, the function of TMEM14A in OV remains unclear. In the present study, it was aimed to find out the roles and underlying mechanism of TMEM14A in OV. RNA interference and lentiviral-mediate vector were used to induce TMEM14A silencing or overexpression. Flow cytometric analysis was used to examine cell apoptosis. Oxygen consumption and extracellular acidification were determined using Seahorse XF24 analyzer. Xenograft mice model was constructed to quantify the role of TMEM14A *in vivo*. Chromatin immunoprecipitation assay was used to determine the connection between TMEM14A and c-Myc. Immunohistochemical staining assay was applied to determine the expression pattern of TMEM14A and c-Myc in OV tissues. TMEM14A was revealed to be highly expressed in OV tumor and correlated with prognostic conditions in patients with OV. TMEM14A inhibited OV cell apoptosis while accelerate their energy metabolism, including glycolysis and oxygen respiration. TMEM14A was positively correlated with c-MYC. Overexpression of c-Myc rescued the function of TMEM14A. In conclusion, TMEM14A was recognized as both diagnostic and prognostic biomarker candidate for early detection of OV and improving the clinical management of patients with OV, which would also facilitate further mechanistic studies of TMEM proteins in OV tumorigenicity. Moreover, the present findings demonstrated that TMEM14A has the potential values as a molecular target in developing the therapy of human OV.

Correspondence to: Dr Jie Chen, Department of Gynecology, The People's Hospital Affiliated to Fujian University of Traditional Chinese Medicine, 817 Middle Road No. 602, Taijiang, Fuzhou, Fujian 350004, P.R. China
E-mail: zqm6488@126.com

Key words: ovarian cancer, transmembrane protein 14A, Wnt/β-catenin, apoptosis, glycolysis, oxygen respiration

Introduction

Ovarian cancer (OV), as a prevalent gynecologic cancer, is among the leading causes of malignancy-related mortality in females across the world (1). It was estimated that there were >200,000 cases and >150,000 OV-related deaths worldwide in 2018 (2,3). OV is associated with high mortality rate and poor prognosis due to its delayed symptom onset, insufficient screening and diagnostic approaches in early stage, and tumor recurrence and metastasis caused by therapy-resistance (3,4). As a matter of fact, the presenting symptoms of OV at early stage remain indistinguishable from the common gastro-intestinal disorders, which minimizes the predictive or detective value in early diagnosis of this type of human cancer (5). For these reasons, OV is accepted as a silent or secret killer for humans, and the development of efficient diagnostic and prognostic bio-markers is crucial for improving early detection and further clinical management of OV in patients (6).

Although the detailed etiology remains not clearly understood, OV tumor display accelerated cell proliferation, diminished cell apoptosis and metabolic reprogramming (7), similar to other types of human cancer. It was reported that the anti-apoptotic protein, B-cell lymphoma 2, is largely overexpressed, along with the presence of survivin and loss of pro-apoptotic receptor CD95, in the late stages of OV (8,9). Moreover, the energy metabolism of OV cells is instrumentally different compared with regular healthy cells in their dominant aerobic glycolysis independent from mitochondrial oxidative phosphorylation (10). This hallmarked glycolytic process supplies the enormous essential materials required for the massive proliferation of OV cells, for example, nucleotides, amino acids, and lipids for DNA replication, protein synthesis, and cell membrane formation, respectively (11). At the meantime, elevated cellular metabolism in OV also influences the mitochondrial-mediated cell apoptosis (7). Additionally, through comparing metabolite profiles, the OV stem cells were revealed undergoing more aggressive glycolytic activities than the differentiated tumor cells, which endow them with the capability of surviving under extreme stress conditions such as like starvation, hypoxia and chemotherapy (7,12).

Transmembrane (TMEM) proteins act as the channel of cells for transportation of cellular materials across membranes and they are also the important components of endoplasmic reticulum, mitochondrial and Golgi membranes (13). Several protein members in TMEM family participate in various biological processes, including autophagy, inflammatory responses, protein glycosylation and drug resistance (14). Most importantly, TMEMs are implicated in the development or regulation of multiple types of human cancer through different mechanisms (14). Certain TMEMs are downregulated or detected with no expression in tumor tissues, such as TMEM7, TMEM25, TMEM97 and TMEM176A, while they inhibit cell proliferation and tumor growth in various types of human cancer (15-18). On the other hand, TMEM16A, TMEM45, TMEM48, TMEM88, TMEM140 and TMEM158 are identified as oncogenes in promoting tumor progression and further metastasis (19-25). These TMEMs are upregulated in different types of human cancer and are associated with the prognostic conditions of patients with cancer (14). TMEM14A is one of them, which localizes in mitochondria, and prior studies have reported its deregulation in hepatocellular carcinoma and colorectal cancer (26,27). Specifically, our previous study also revealed the pro-tumorigenic functions of TMEM14A in regulating cell cycle, proliferation, invasion and metastatic pathways in OV (28). However, its biological roles in programmed cell death and cellular respiration have not been fully understood.

In the present study, it was designated to explore the relationship between TMEM14A and prognosis in patients with OV, the functions of TEME14A in OV cellular activities particularly cell apoptosis and energy metabolism, as well as the underlying mechanisms of its bio-functions. It was demonstrated that the expression of TMEM14A in OV tumorous tissues is elevated, and its expression is positively correlated with the mortality rate of patients with OV. Further, through establishing TMEM14A silencing and overexpression in OV cells, our findings revealed that knockdown of TMEM14A contributed to suppress the growth of human OV cells through blocking the activity of glycolysis. Thus, the present study established the recognition of TMEM14A in OV development and offered a potential target for both diagnosis and treatment of OV.

Materials and methods

Human ovarian tissue collection. A total of 25 pairs of human OV tumorous tissues and para-carcinoma tissues were collected from June 2019 to October 2021) and used to examine the expression level of TMEM14A. The patients were selected using the following inclusion criteria: Age was over 18 years and with a primary epithelial tumor of the ovary. Patients were excluded if they had non-epithelial ovarian tumors or had non-primary (metastatic or recurrent) tumor of the ovary. Moreover, a total of 120 patients (including II: 65, III-IV: 55) with OV participated in a prospective study. Patients were interviewed by clinicians at participating hospitals, and patient reported and clinical variables were recorded in a standardized questionnaire. The Kaplan-Meier method was used to evaluate overall survival. All the samples were provided by The People's Hospital Affiliated to Fujian University of traditional Chinese Medicine (Fuzhou, China). Written informed consent was provided from all patients enrolled in the present study. The research protocol was approved (approval no. 2019-017-02) by the ethics committee of People's Hospital Affiliated to Fujian University of traditional Chinese Medicine (Fuzhou, China) according to the Declaration of Helsinki.

Cell culture. Cell lines (A2780, SKOV3 and CAOV3) were purchased from the cell bank of Shanghai Biology Institute. Cells were cultured in DMEM (Trueline) with the supplementation of 2 mM l-glutamine, 10% FBS (Thermo Fisher Scientific, Inc.), and 1% penicillin/streptomycin (Beijing Solarbio Science & Technology Co., Ltd.), maintained at 37˚C with 5% CO_2. The Wnt/β-catenin inhibitor XAV9390 (cat. no. S1180; Selleck Chemicals) was dissolved in DMSO (cat. no. D2650; Sigma-Aldrich; Merck KGaA) and used to inhibit the activity of Wnt/β-catenin pathway in the aforementioned human OV cell lines.

Reverse transcription-quantitative PCR (RT-qPCR). TRIzol® reagent (Invitrogen; Thermo Fisher Scientific, Inc.) was used for the extraction of total RNA from OV cells and collected samples. Then, cDNA synthesis kit (Thermo Fisher Scientific, Inc.) was used to reversely transcribe the extracted RNA (1 ng/μl) into cDNA following the manufacturer's protocol. Subsequently, qPCR was performed using a SYBR Premix Ex Taq II with Tli RNaseH (Takara Bio, Inc.) on an ABI Prism 7500 system (Thermo Fisher Scientific, Inc.). The target genes were individually normalized to β-actin. The relative transcript level of the target gene was estimated using the $2^{-\Delta\Delta Cq}$ method (29). All the data were presented as the mean value from triplicate. The thermocycling conditions were as follows: 95˚C for 10 min; followed by 40 cycles at 95˚C for 15 sec and 60˚C for 45 sec and final extension at 72˚C for 60 sec. The sequences of the primers for qPCR were as follows: TMEM14A forward, 5'-TGGATA TAAGCGGAGAGG-3' and reverse, 5'-CCATTACAGCAG GATGAC-3'; β-catenin forward, 5'-TGGCAGCAACAGTCT TAC-3' and reverse, 5'-GCCCTCATCTAATGTCTCAG-3'; lactate dehydrogenase (LDH) A forward, 5'-CCTGTATGG AGTGGAATG-3' and reverse, 5'-GGATGTGTAGCCTTT GAG-3'; and GAPDH forward 5'-AATCCCATCACCATC TTC-3' and reverse, 5'-AGGCTGTTGTCATACTTC-3'.

Western blotting. Radioimmunoprecipitation lysis buffer [JRDUN Biotechnology (Shanghai) Co., Ltd.] containing Protease Inhibitor Cocktail without EDTA (Roche Diagnostics GmbH) was used for the extraction of total proteins. The enhanced bicinchoninic acid assay kit (Thermo Fisher Scientific, Inc.) was used to estimate the concentration of the total proteins. The extracted proteins with equal amounts of 25 μg were separated using 10% sodium dodecyl sulphate-polyacrylamide gel electrophoresis and then transferred overnight to a nitrocellulose membrane (MilliporeSigma). The transferred membrane was blocked with 5% non-fat dry milk at room temperature for 1 h and overnight probed by different primary antibodies at 4˚C, followed by 1 h of incubation with the secondary antibody (1:1,000; cat. no. A0208, anti-rabbit IgG; Beyotime Institute of Biotechnology) at 37˚C. The detection of the expression value of proteins was performed using

an enhanced system for chemiluminescence (Tanon Science and Technology Co., Ltd.). The primary antibodies used were as follows: GAPDH (1:5,000; cat. no. 60004-1-1G; ProteinTech Group, Inc.), β-catenin (1:5,000; cat. no. ab32572), C-myc (1:500; cat. no. ab39688), LDHA (1:1,000; cat. no. ab101562), survivin (1:5,000; cat. no. ab469) and TMEM14A (1:1,000; cat. no. ab236904; all from Abcam). The intensities of the signals were determined using a using the Bio-Rad Universal Hood II Gel Doc 2000 Imaging system (Bio-Rad Laboratories, Inc.) and the gray value was analyzed using ImageJ v. 1.8.0.112 (National Institutes of Health) after being visualized with an electrochemiluminescence kit (Wuhan Boster Biological Technology Ltd.).

TMEM14A silencing and overexpression. TMEM14A was induced silencing and overexpression using RNA interference (RNAi) or lentiviral-mediator vector according to the previously described method (28). Briefly, Lentiviral plasmid (pLKO.1) with siRNAs (1,000 ng) targeting three distinctive regions of human TMEM14A (NM_014051), including siTMEM14A-1: TAGCACTGTCACCTCTAA TAT; siTMEM14A-2, AAGCTTAAACTACAACTTGTC; siTMEM14A-3, AAGTGGAGTTCACAGAATGAT] and siRNA negative control (siNC: CCTAAGGTTAAGTCG CCCTCG) were constructed (Shanghai Majorbio Bio-pharm Technology Co., Ltd.). Lentiviral plasmid (pLVX-puro) with human TMEM14A complete sequence or a mock plasmid for negative control (oeNC) was also constructed. Overexpressing lentivirus plasmid pLVX-Puro (Clontech; Takara Bio USA, Inc.) was generated by cleavage of the pLVX-Puro plasmid using EcoR I/BamH I. Lentivirus packaging was performed using the second-generation lentivirus packaging kit (Addgene, Inc.), pLVX-Puro-TMEM14A (1,000 ng), psPAX2 (packaging vector, 100 ng), pMD2G (envelope vector, 900 ng) and incubated with 1 ml of Lenti-Easy Packaging Mix (Shanghai GeneChem Co., Ltd.) for 15 min at 37˚C. The mixture was then incubated for another 20 min in Lipofectamine 2000 (Invitrogen; Thermo Fisher Scientific, Inc.) at 37˚C following the manufacturer's instructions. All the following experiments were conducted after 48 h post-transfection. It was applied into 293T cell (American Type Culture Collection) culture medium for 6 h at 37˚C. Subsequently, 293T cells were seeded ($2x10^5$ cells/well) in a 12-well plate and cultured to 80% confluence. After incubation in serum-free DMEM for 4 h, cells were transfected as aforementioned with lentiviruses for 3 days. Transfected cells were filtered using a 0.45 μM mesh, which were concentrated at 70,000 x g at 4˚C for 2 h. The supernatant was collected for detecting viral titers. The CAOV3 cells were cultured with diluted lentiviruses and screened the lentivirus transfection rate at 72 h. The transfection efficacy of TMEM14A was finally examined by using RT-qPCR once the lentivirus transfection rate was over 80%.

Cell proliferation. To examine the function of TMEM14A in OV cell proliferation, Cell Counting Kit-8 (CCK-8) assay (SAB Biotherapeutics, Inc.) was performed according to the manufacturer's protocol. In brief, cells ($2x10^3$) were seeded in 96-well plates and maintained for 0, 12, 24 and 48 h at 37˚C. Then, cells were incubated with CCK-8 solution (1:10) for 1 h. The OD values at 450 nm were measured by a microplate reader (Beijing Pulang New Technology Co., Ltd.). Triplicate tests were needed for each time.

Cell apoptosis. Cell apoptosis was evaluated usingAnnexin V-FITC/PI staining (cat. no. C1062; Beyotime Institute of Biotechnology) after viral infection for 48 h following the manufacturer's protocol. Cells ($5x10^4$) were collected by centrifugation at 1,000 g for 5 mins at room temperature. Then, the positive-stained cells were determined by a flow cytometer (BD Biosciences). CytExpert software 2.0 (Beckman Coulter, Inc.) was used for analysis. Annexin V-FITC$^+$ and PI$^-$ populations indicated apoptosis. Annexin V$^-$ and PI$^-$ populations were healthy cells that were considered negatively stained. Annexin V$^+$ and PI$^-$ cells indicated cells in early apoptosis. Moreover, Annexin V$^+$ and PI$^+$ staining indicated cells in necrosis (post-apoptotic necrosis or late apoptosis). All the data were presented as the mean from triplicate.

Immunofluorescent staining. Paraffin-embedded OV tissues wax blocks were cut into 4-μm thick tissue pieces and placed on glass sides. Slides were then subjected to immunohistochemical (IHC) staining to evaluate Ki-67 expression. Slides were were dehydrated twice in anhydrous ethanol for 5 min, 85% ethanol for 5 min and 75% ethanol for 5 min. After washing in ddH_2O, sections were immersed in citrate buffer (pH 6.0; cat. no. E673000; Sangon Biotech Co., Ltd.) for 15 min antigen retrieval at room temperature. They were incubated in 3% H_2O_2 in the dark for 25 min at 37˚C and blocked in 3% BSA (Sangon Biotech Co., Ltd.; cat. no. E661003) at 37˚C for 30 min. Then slides were incubated with Ki-67 primary antibodies (1:100; cat. no. 27309-1-AP; ProteinTech Group, Inc.) in a humidified chamber overnight at 4˚C. Slides were then washed 3 times with PBS before they were incubated with Alexa Fluor 488-conjugated goat anti-rabbit IgG (H + L) secondary antibody (1:200; cat. no. A0423; Beyotime Institute of Biotechnology) for 1 h at 4˚C in darkness. Next, slides were stained with 4',6-diamidino-2-phenylindole (DAPI, 1:400 dilution) to visualize the nuclei. Finally, slides were sealed by anti-fluorescence quenching seal tablet (cat. no. G1401; Wuhan Servicebio Technology Co., Ltd.) before they were observed and images captured under a laser scanning confocal microscope (NIKON ECLIPSE C1; Nikon Corporation) and an imaging system (NIKON DS-U3; Nikon Corporation).

In vitro measurements of oxygen consumption and extracellular acidification. Seahorse XF24 analyzer (Agilent Technologies, Inc.) was used to measure the oxygen consumption rate (OCR) and extracellular acidification rate (ECAR) of human OV cells. In this case, OV cells ($5x10^5$) were plated in DMEM supplemented with 10% human serum in six-well plates for 24 h.

For each assay, after treatment, cells were counted and equal number of viable cells were used and plated onto XF microplates coated with Cell-Tak (BD Biosciences) and allowed to adhere for 4-6 h. DMEM medium was replaced with XF base (OCR) or glycolysis base (ECAR) media. A total of 3 technical replicates for each condition were plated. Oligomycin (an ATP coupler) was added, followed by FCCP (an ETC accelerator), which was then analyzed using Seahorse XFp 24 (Agilent Technologies, Inc.). Increase in OCR above basal respiration

after FCCP addition is spare respiratory capacity while total is maximal respiratory capacity. ECAR was measured under basal condition which increases after addition of glucose that provides glycolytic flux. Addition of oligomycin measures the glycolytic capacity.

In brief, all the measurements were performed by using and following the manufacturer's protocol. Data were analyzed based on the XF24 Software and Operation Manual from Seahorse.

Dual-luciferase reporter gene assay. Potential binding sites for c-Myc in the TMEM14A promoter were predicted using GeneCards database (www.genecards.org). According to the predictions, DNA fragments containing wild-type (WT) or mutant sequences for c-Myc binding were synthesized and cloned into luciferase reporter vectors (pGL3-Basic; Addgene, Inc.). These constructs (namely, WT and Mut promoter), were introduced with an internal reporter plasmid and oec-Myc into human CAOV3 cells by using Lipofectamine 2000 (Invitrogen; Thermo Fisher Scientific, Inc.) for 48 h and luciferase activities were measured 48 h after transfection using a dual-luciferase reporter gene kit (Beijing Yuanpinghao Biotechnology Co., Ltd.). Firefly luciferase activity was normalized to Renilla luciferase activity. Relative Firefly and Renilla luciferase activities were measured using the Dual-Luciferase Reporter Gene Assay kit (Promega Corporation).

Xenograft mice model. The animal trial was approved by the ethics committee of People's Hospital Affiliated to Fujian University of traditional Chinese Medicine (Fuzhou, China) and conducted following the guidelines of the institute. All the animals involved in the present study were husbanded and treated following the guidelines of Institutional Animal Care and Use Committee (IACUC). All the animal work took place in The People's Hospital Affiliated to Fujian University of traditional Chinese Medicine (Fuzhou, China). Nude mice (4-5 weeks-old; weight, 18-22 g; n=36) were purchased from Shanghai Laboratory Animal Company. Equal amounts of ~$2x10^6$ A2780 cells with siNC- and siTMEM14A transfection or CAOV3 with oeNC or oeTMEM14A were subcutaneously injected into the mice (n=6/group) at the right flank. After injection, the animals were housed at the condition of 21˚C, 45-55% humidity with 12-h light/dark cycles, with lights on at 7:00 am. Standard food and filtered water were available *ad libitum*. The weight and growth status of the mice were monitored every day. After 12 days, the volumes of the tumors were measured every 3 days using a vernier caliper until the experiment had reached 33 days. Then, mice were euthanized with intraperitoneal injection of 120 mg/kg sodium pentobarbital before the tumor was removed. The hearts of the mice were then monitored, and death was confirmed by cardiac arrest. Tumor volume was calculated as follows: Tumor volume (mm^3)=Tumor length (mm) x Tumor width $(mm)^2/2$. All the tumor tissues were then fixed by 4% formalin for 30 min at 4˚C and used in the following analyses.

IHC assay. The tumorous or normal OV tissue sections (4-7 μm in thickness) were incubated with TMEM14A (1:350, cat. no. PA5-112745; Thermo Fisher Scientific, Inc.) or c-MYC (1:1,000; cat. no. D84C12; Cell Signaling Technology, Inc.) antibodies overnight at 4˚C, followed by incubation with HRP-labeled secondary antibodies (cat. no. D-3004; Long Island Biotech) for 30 min at 25˚C. For IHC staining, 3,3'-diaminobenzidine (DAB) substrate (Shanghai Long Island Biotechnology Co., Ltd.) and hematoxylin 714094 (BASO Diagnostic Inc.) were used. The ECLIPSE Ni-E/Ni-U microscope with DS-Ri2 imaging system (Nikon Corporation) was used to visualize TMEM14A or c-Myc-positive cells. The results were read by two independent pathologists according to a previous report (30). Stain intensity and the percentage of positive cells were scored as follows: i) for stain intensity, negative, score 0; light brown, score 1; brown, score 2; deep brown, score 3; ii) for percentage of positive cells, scored each criterion on a scale of 0 to 3, ≤5%, scored 0; 6-25% scored 1, 26-50% scored 2 and >50% scored 3. The final IHC-score (0-9) were calculated by multiplying the scores of the percentage of positive cells by the stained intensity.

Chromatin immunoprecipitation (CHIP) assays. A total of $4x10^6$ human CAOV3 cells were used in this section. Firstly, CAOV3 cells were cross-linked by 1% formaldehyde and then stopped by using glycine solution (125 mM; cat. no. 161-0718; Bio-Rad Laboratories, Inc.). After that, cells were washed with cold PBS for 2 times and then sonicated at the condition of 4.5 sec impact, 9 sec per interval, 14 times in total to collect adequate fragment sizes of DNA. Total genomic DNA was collected by using SimpleChIP® Plus Sonication Chromatin IP kit (cat. no. 56383; Cell Signaling Technology, Inc.) according to the manufacturer's protocol. ChIP was carried out with anti-c-Myc antibody (cat. no. 8173) or anti-IgG (2729; both from Cell Signaling Technology, Inc.). DNA was eluted and purified, analyzing the presence of previously identified putative antioxidant response elements by RT-qPCR with specific primers. Three independent immunoprecipitations were needed for each sample.

Terminal deoxynucleotidyl transferase dUTP nick end labeling (TUNEL). TUNEL for collected tissue sections was conducted using an Tunel kit (cat. no. 11684817910; Roche Diagnostics), principally following the instructions of the supplier, and the cell counting was performed in triplicate. Cells were cultured in 24-well plates ($1x10^5$ cells per well) and fixed with 4% paraformaldehyde for 15 min at 25˚C. TUNEL solution was added to each well at 37˚C for 60 min. After rinsing with PBS, the cells were stained with DAPI (1:500) for 5 min at 37˚C. The slides were mounted using Fluoromount-G™ (Thermo Fisher Scientific, Inc.). A total of 3 random fields of view were captured with a fluorescence microscope (Olympus Corporation) and the percentage of TUNEL-positive cells was calculated.

Statistical analyses. All the data analyses were conducted using GraphPad software (version 7.0; GraphPad Software, Inc.). Data expressed as the mean ± standard deviation from at least triplicate. One-way ANOVA was performed for multiple comparisons among groups using the Tukey's multiple comparisons test. $P<0.05$ was considered to indicate a statistically significant difference.

Results

Highly expressed TMEM14A in OV is correlated with the poor prognosis of patients with OV. In order to investigate

Table I. Correlation between TMEM14A expression and clinicopathological features in 120 patients with ovarian cancer.

Parameters	Group	N	Expression level of TMEM14A		P-value
			Low	High	
Age, years					No significance
	<60	69	32	37	
	≥60	51	21	30	
Tumor size, cm					0.0462
	≤4	78	50	28	
	>4	42	19	23	
T stage					0.0053
	II	65	17	48	
	III-IV	55	28	27	
Recurrent					<0.001
	Negative	74	46	28	
	Positive	46	10	36	

TMEM14A, transmembrane protein 14A.

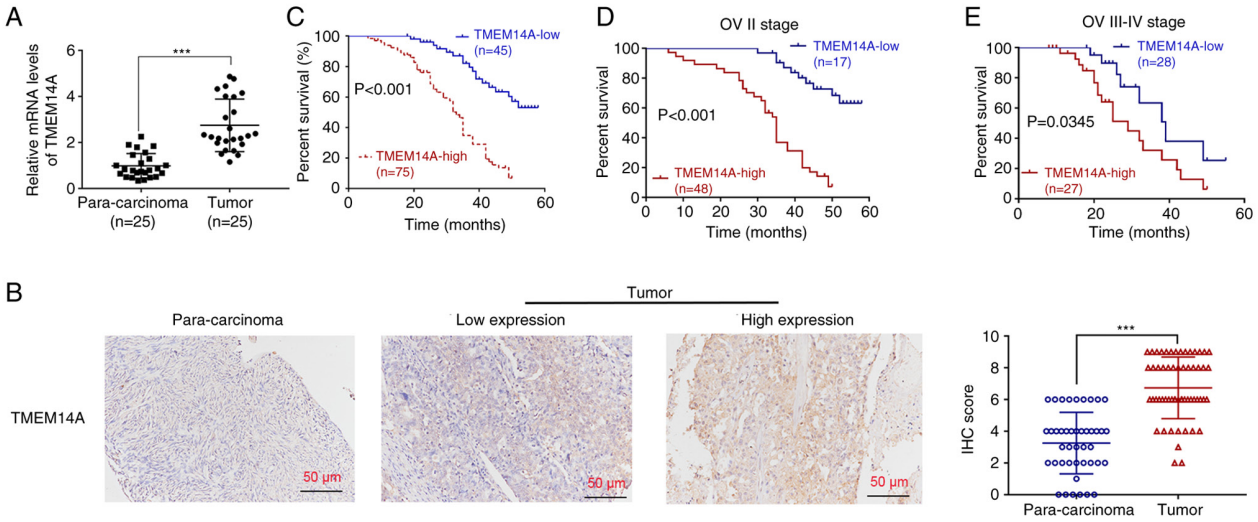

Figure 1. Upregulation of TMEM14A in OV tissues and its correlation with prognosis of patients with OV. (A) The relative mRNA levels of TMEM14A in paired (n=25) human OV tumorous and para-carcinoma tissues. (B) Immunohistochemical staining assay was used to examine the protein expression of TMEM14A in para-carcinoma and OV tissues (Scale bar, 50 μm). (C) Correlation between TMEM14A high (n=75) or low (n=45) levels and survival probability of patients with OV. (D) Correlation between TMEM14A high (n=48) or low (n=17) levels and survival probability of patients with OV at stage II. (E) Correlation between TMEM14A high (n=27) or low (n=28) and survival probability of patients with OV at stage III-IV. ***P<0.001. TMEM14A, transmembrane protein 14A; OV, ovarian cancer.

the relationship between TMEM14A and OV, the expression levels of TMEM14A in paired tumorous and para-carcinoma tissues from patients with OV were analyzed. It was observed that the relative mRNA level of TMEM14A was significantly (P<0.001) higher in the tumorous OV tissues in comparison with that in the adjacent tissues (Fig. 1A). Next, IHC assay was used to examine the protein expression ofTMEM14A in tumor and para-cancerous tissues. In 93 patients, 40 tumorous tissues were observed to exhibit high level ofTMEM14A expression, whereas 53 tissues were identified with low level of TMEM14A expression (Fig. 1B). Moreover, the overall survival rate of 120 patients with OV (including II stage: 65, III-IV stage:55) were examined by using the Kaplan-Meier method. The related clinicopathological features of patients are listed in Table I. The results suggested that high expression of TMEM14A is positively correlated with the tumor size, tumor stage and recurrence, while not identified in age of patients with OV. A significantly lower survival rate was observed in OV patients with high expression of TMEM14A compared with that observed in patients with low TMEM14A expression throughout the 60-month experiment duration (Fig. 1C). More importantly, the correlation between TMEM14A and prognosis of patients with OV showed a higher significance at stage II compared with that in stage III-IV (Fig. 1D and E).

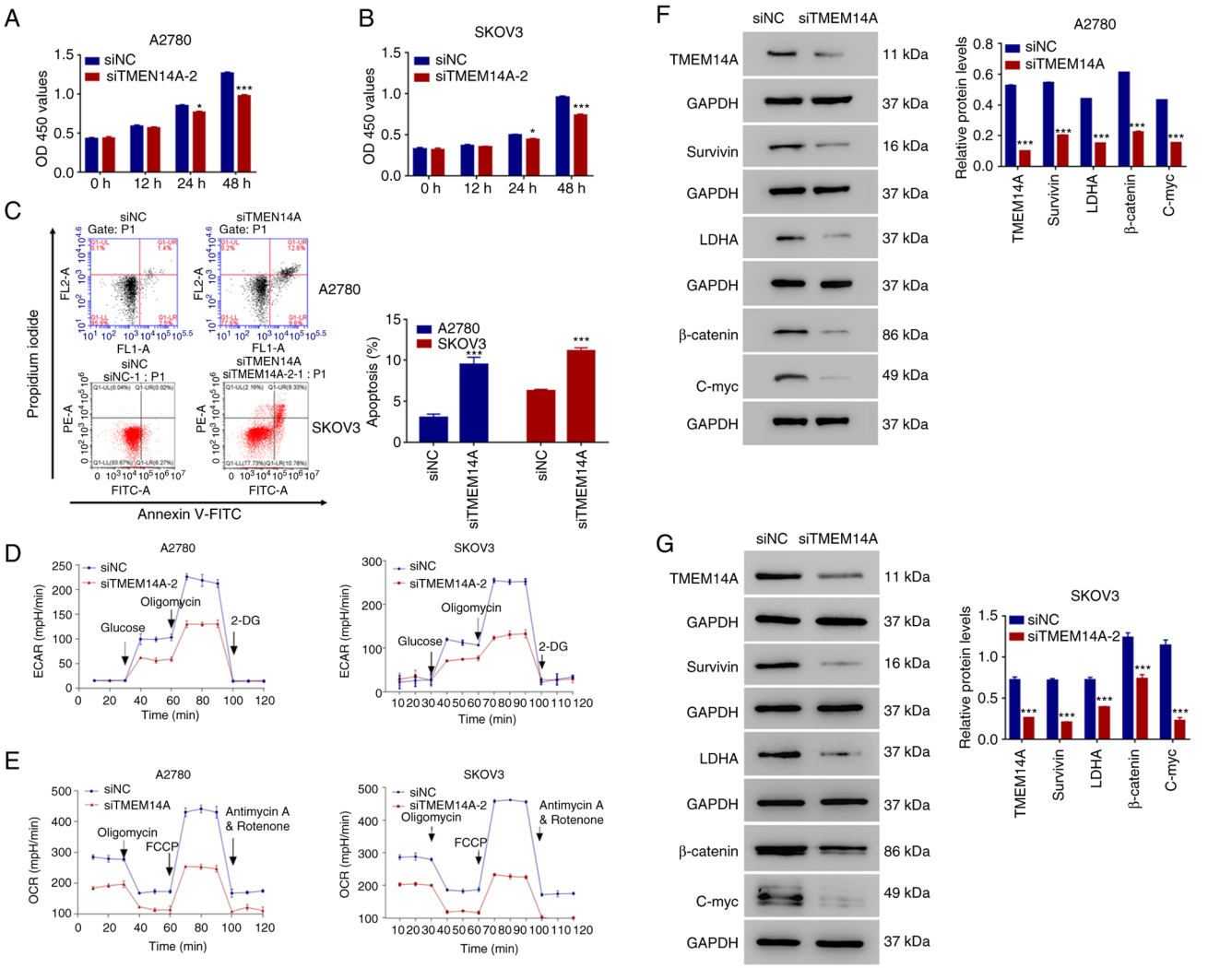

Figure 2. Effects of TMEM14A silencing on apoptosis and metabolism of ovarian cancer cells. A2780 and SKOV3 cells were transfected with siNC or siTMEM14A-2. (A and B) Proliferation of (A) A2780 and (B) SKOV3 cells. (C) Cell apoptosis. (D) ECAR. (E) OCR. (F and G) Western blot quantification of protein expression levels of TMEM14A, survivin, LDHA, β-catenin and c-Myc in (D) A2780 and (E) SKOV3 cells. *P<0.05, ***P<0.001 vs. siNC. TMEM14A, transmembrane protein 14A; si-, small interfering; NC, negative control; ECAR, extracellular acidification rate; OCR, oxygen consumption rate; LDHA, lactate dehydrogenase A.

TMEM14A knockdown promotes cellular apoptosis but inhibits energy metabolism of OV cells. TMEM14A gene was further silenced in A2780 and SKOV3 cells for exploring its functions in human OV. As revealed in Fig. 2A and B, the proliferation of A2780 and SKOV3 cells was significantly decreased after transfection with siTMEM14A. Moreover, the apoptotic rates of both cells with TMEM14A knockdown were significantly (P<0.001) promoted compared with those in the control cells (Fig. 2C). Furthermore, glycolysis (Fig. 2D) and oxygen respiration (Fig. 2E) in TMEM14A-silenced A2780 and SKOV3 cells were markedly reduced, reflected by the declined ECAR and OCR, respectively, in comparison with those in the control cells. In addition, through western blot analysis, it was detected that TMEM14A silencing could also induce significant (P<0.001) downregulation of the cellular protein levels of survivin, LDHA, β-catenin and c-Myc in A2780 (Fig. 2F) and SKOV3 (Fig. 2G) cells.

TMEM14A silencing suppresses tumorigenicity of OV in mice. The *in vivo* functions of TMEM14A in OV development was further evaluated based on mice model. The volume of tumor collected from the mice injected with TMEM14A-silenced A2780 cells was significantly (P<0.01) decreased after 24 days until 33 days (Fig. 3A). Similarly, at the 33rd day, the weight of tumor collected from the mice injected with TMEM14A-silenced A2780 cells was also significantly (P<0.001) decreased (Fig. 3B). Moreover, the positive Ki-67 staining cells were significantly downregulated in siTMEM14A-injected tumor (Fig. 3C). Using TUNEL assay, the significantly (P<0.001) elevated cell apoptotic rate in tumors collected from the mice injected with TMEM14A-silenced A2780 cells (Fig. 3D) could be detected. Additionally, the protein levels of TMEM14A, survivin, LDHA, β-catenin and c-Myc were also found to be significantly (P<0.001) lower in tumors collected from the mice injected with TMEM14A-silenced A2780 cells, when compared with those in collected tumors from the control mice (Fig. 3E).

TMEM14A promotes OV in vitro possibly through regulating Wnt/β-catenin pathway. Gene enrichment analysis indicated

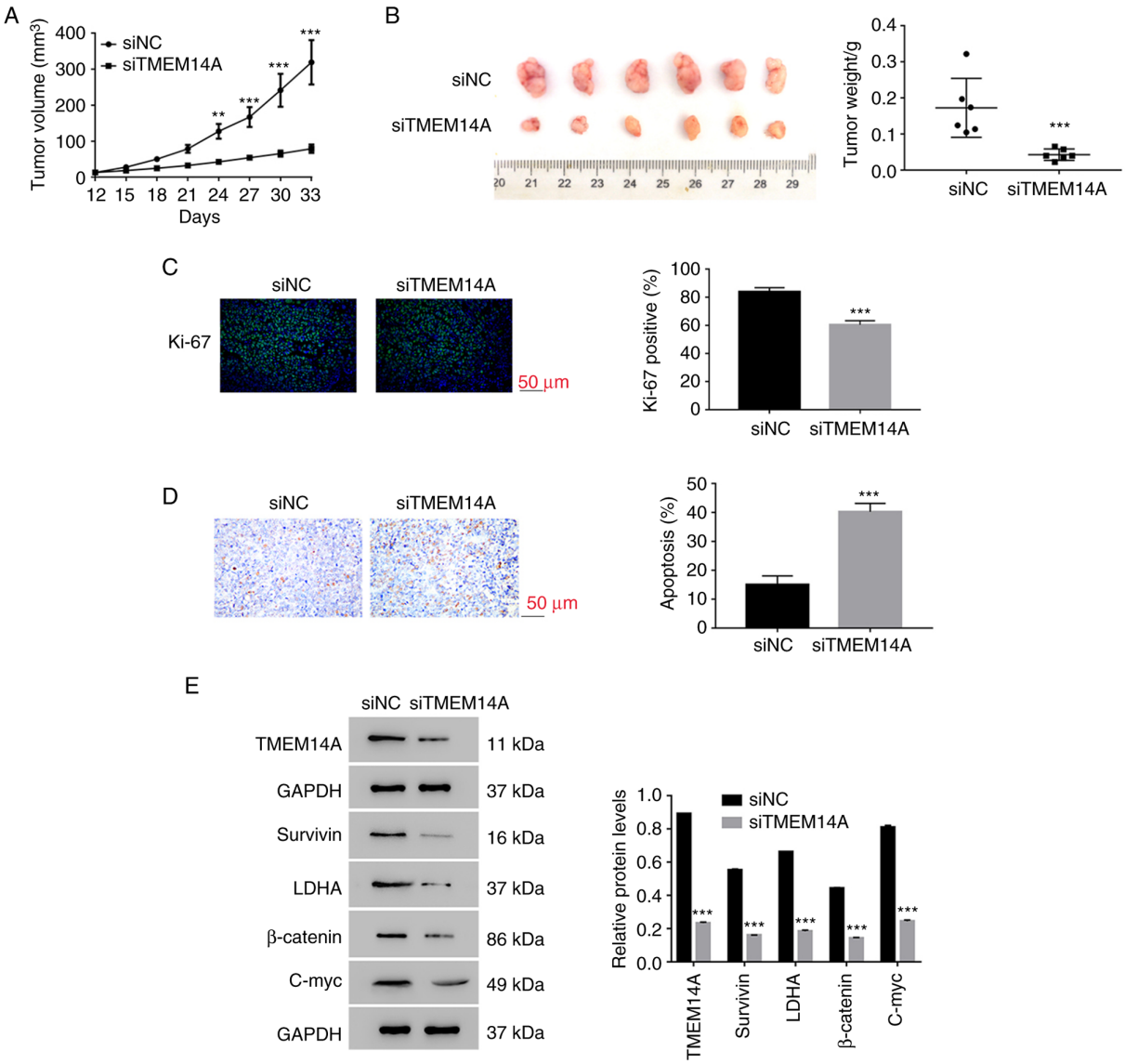

Figure 3. Effects of TMEM14A silencing on tumorigenicity of ovarian cancer *in vivo*. Nude mice (n=6/group) were injected with siNC or siTMEM14A-transfected A2780 cells. (A) Tumor volume. (B) Tumor weight. (C) Ki-67 staining assay was used to examine the proliferation of siNC or siTMEM14A tumor. (D) TUNEL staining and correspondent quantification of apoptotic ratio of murine tumors. (E) Western blot protein quantification of the expression levels of TMEM14A, survivin, LDHA, β-catenin and c-Myc in murine tumors. **P<0.01 and ***P<0.001 vs. siNC. TMEM14A, transmembrane protein 14A; si-, small interfering; NC, negative control; LDHA, lactate dehydrogenase A.

that TMEM14A is positively correlated with Wnt/β-catenin pathway in OV (Fig. S1C). To further examine this relationship, TMEM14A overexpression was induced in CAOV3 cells (Fig. 4A and B). The apoptotic rate of CAOV3 cells with TMEM14A overexpression was significantly (P<0.05) suppressed, compared with that in the control cells (Fig. 4C). Moreover, ECAR indicating glycolysis (Fig. 4D) and OCR indicating oxygen respiration (Fig. 4E) in TMEM14A-overexpressed CAOV3 cells were markedly elevated, in comparison with those in the control cells. In addition, the overexpression of TMEM14A also induced significant (P<0.001) upregulation of the cellular survivin, LDHA, β-catenin and c-Myc protein levels in CAOV3 cells (Fig. 4F).

At the other hand, the CAOV3 cells with or without TMEM14A overexpression were treated by Wnt/β-catenin inhibitor XAV9390, to explore the underlying mechanism in OV-promotive effect of TMEM14A. It was observed that XAV9390 treatment could significantly (P<0.001) stimulate cell apoptosis (Fig. 4C), decrease ECAR (Fig. 4D) and OCR (Fig. 4E), and downregulate related protein (survivin, LDHA, β-catenin and c-Myc) levels in CAOV3 cells (Fig. 4F). Furthermore, the Wnt/β-catenin inhibitor XAV9390 was also capable of significantly (P<0.001) counteracting the aforementioned OV-promotive effects of TMEM14A overexpression, including partially rescuing cell apoptosis (Fig. 4C), energy metabolism (Fig. 4D and E) and related protein levels (Fig. 4F).

The glycolysis inhibitor 2-deoxyglucose (2-DG) suppresses the function of TMEM14A in human OV cells. More importantly, functional analysis also demonstrated that TMEM14A is also positively correlated with glycolysis metabolism (Fig. S1A). To further examine the function of TMEM14A in the glycolysis of human OV cells, the glycolysis inhibitor

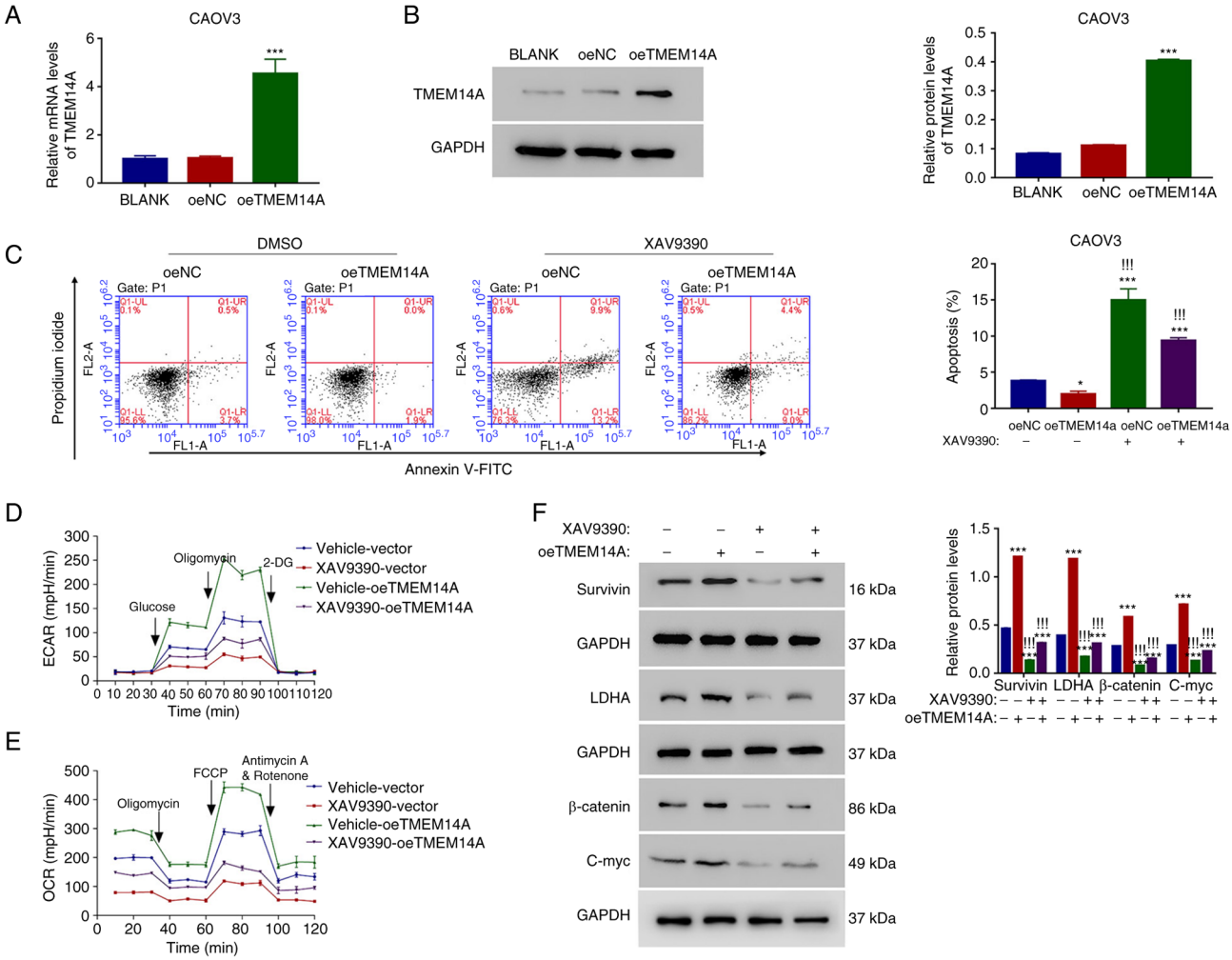

Figure 4. Effects of TMEM14A overexpression and Wnt/β-catenin inhibitor XAV9390 in ovarian cancer cells. CAOV3 cells were transfected with oeTMEM14A. (A) The relative transcriptional level of TMEM14A. (B) The protein level of TMEM14A. (C) Cell apoptosis. (D) ECAR. (E) OCR. (F) Western blot protein quantification of the expression levels of survivin, LDHA, β-catenin and C-myc. *P<0.05 vs. oeNC; ***P<0.001 vs. oeNC; $^{!!!}$P<0.001 vs. oeTMEM14A. TMEM14A, transmembrane protein 14A; ECAR, Extracellular acidification rate; OCR, Oxygen consumption rate; oe, overexpression; NC, negative control; LDHA, lactate dehydrogenase A.

2-DG was used to block the activity of glycolysis in human OV cells that transfecting with oeNC or oeTMEM14A. As revealed in Fig. 5A, overexpression of TMEM14A significantly suppressed the apoptosis of human CAOV3 cells, while this function was significantly abolished by the inhibitor 2-DG. Moreover, the 2-DG also deeply suppressed the proliferation of oeTMEM14A-transfecting CAOV3 cells (Fig. 5B). Importantly, both the activity of ECAR and OCR of oeTMEM14A-transfected cells were also significantly suppressed in the presence of the inhibitor 2-DG (Fig. 5C and D). Furthermore, results obtained *in vivo* suggested that the glycolysis inhibitor 2-DG significantly suppressed the tumor volume and weight of oeTMEM14A tumor (Fig. 5E-G). More importantly, Ki-67 staining assay indicated that the inhibitor 2-DG significantly suppressed the proliferation of CAOV3 cells in oeTMEM14A tumor *in vivo*. Collectively, all results indicated that the function of TMEM14A was suppressed by the inhibitor 2-DG both *in vitro* and *in vivo*.

c-Myc is positively correlated with TMEM14A in OV tissues. To explore the promoter of TMEM14A, c-Myc is discovered as a transcript factor. The present results suggested that TMEM14A is upregulated in oec-Myc-transfected cells (Fig. S2A-D). Once mutating the binding site of TMEM14A for c-Myc, the promoter activity of TMEM14A was deeply suppressed in oec-Myc-transfected cells (Fig. S2E). Results obtained from CHIP assay demonstrated that c-Myc could bind on the promoter region of TMEM14A (Fig. S2F). Clearly, knockdown of TMEM14A significantly inhibited the proliferation and ECAR value in human OV cells, while these effects were remarkably rescued after transfecting with oec-Myc (Fig. S2G and H). Notably, correlation analysis suggested that the expression of c-Myc is positively correlated with TMEM14A in human OV tissues (Fig. S2I and J). Taken together, these results demonstrated that c-Myc is involved in the molecular network of TMEM14A in human OV tissues.

Discussion

According to previous studies, the upregulation of TMEM14A is associated with colorectal cancer and hepatocellular carcinoma, which serves as a tumor marker candidate in predicting

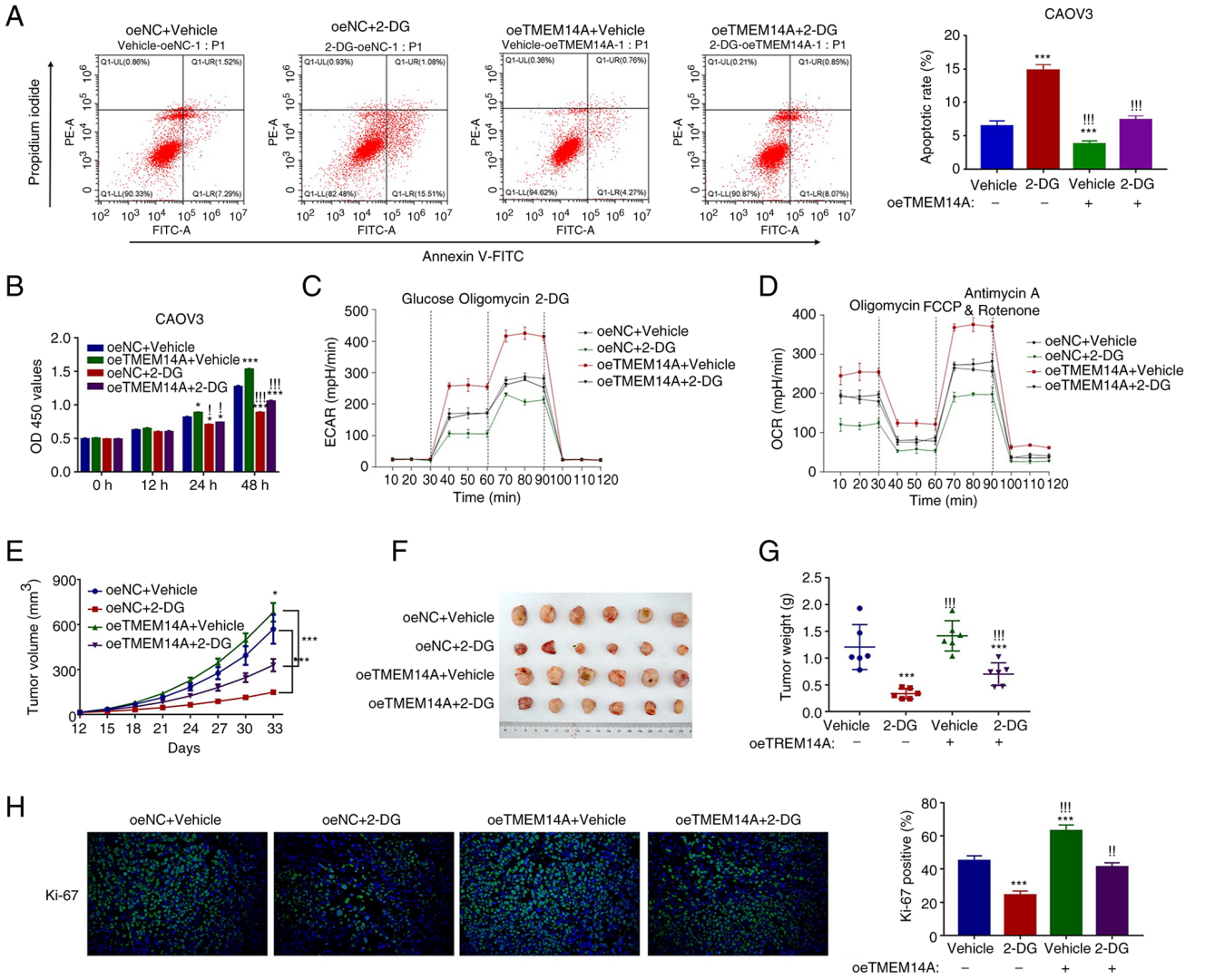

Figure 5. Glycolysis inhibitor 2-DG disrupts the function of TMEM14A in human ovarian cancer cells. (A) The inhibitor 2-DG promoted the apoptosis of human CAOV3 cells after transfection with oeNC or oeTMEM14A. (B) The inhibitor 2-DG decreased the proliferation of CAOV3 in oeNC or oeTMEM14A transfected cells. (C and D) The inhibitor 2-DG decreased the activities of (C) ECAR and (D) OCR in oeNC or oeTMEM14A transfected cells. (E-G) Both the (E and F) tumor volume and (G) weight of oeNC and oeTMEM14A were suppressed by the inhibitor 2-DG. (H) Ki-67 staining assay was used to examine the proliferation of tumors as aforementioned. *P<0.05, ***P<0.001 vs. oeNC + Vehicle; $^{!}$P<0.05, $^{!!}$P<0.01 and $^{!!!}$P<0.001 vs. oeTMEM14A + Vehicle. 2-DG, 2-deoxyglucose; oe, overexpression; NC, negative control; TMEM14A, transmembrane protein 14A; ECAR, Extracellular acidification rate; OCR, Oxygen consumption rate.

recurrence (26,27). Meanwhile, our previous bioinformatics study also revealed that TMEM14A is overexpressed in OV tissues (28). Accordingly, in the present study, through analyzing the paired tumorous and adjacent tissues in patients with OV, it was also confirmed that TMEM14A is highly expressed in tumorous OV tissues. Furthermore, it was also demonstrated that the high expression of TMEM14A in patients with OV is tightly connected with their high mortality rate, indicating the potential of TMEM14A as an efficient prognostic biomarker for OV.

Apoptotic program exists in all types of cells, whereas the resistance towards apoptosis is one of the critical trademarks of OV cells, which contributes to their chemoresistance and tumor recurrence (31). Therefore, various drugs are targeting apoptotic pathways in OV for its current clinical therapies (32). In the current study, it was observed that TMEM14A overexpression in OV cells suppressed their apoptotic process, while TMEM14A knockdown could induce high rates of cellular apoptosis both *in vitro* and *in vivo* in murine OV tumor. These findings revealed that TMEM14A plays an important role in OV by influencing its apoptotic program, which is supported by the previous study (32) demonstrating that TMEM14A could suppress cell apoptosis by stabilizing mitochondrial membrane potential. Moreover, survivin is one of the apoptotic inhibitor proteins which blocks apoptotic process in cells through inhibiting caspase-9 and its antagonists are beneficial for OV therapies (33). Accordingly, it was detected that TMEM14A could also affect the cellular level of surviving, through which it ultimately regulated the apoptotic rate of OV cells.

Cancer cells reply on glycolysis for sustaining their enormous demands for cell proliferation and evading signals that trigger cell death (34). At the same time, their oxidative phosphorylation is independent from the elevated glycolytic

activities, which is also accelerated in the cancer cells (35). The measurement of ECAR and OCR is considered as the most powerful method for monitoring cellular glycolytic and respiratory rates (36). It was demonstrated that TMEM14A knockdown and overexpression could inhibit and promote both ECAR and OCR in OV cells, respectively, indicating its pro-oncogenic functions in motivating both glycolysis and oxygen respiration. On the other hand, LDH is the critical enzyme functioning in the metabolic reprogramming of tumor cells, which converts pyruvate into lactate and regulates the exchange of nutrients (37). Moreover, LDH is elevated in the peritoneal fluid of OV and it is correlated with the clinical stage and grade of OV (38,39). In the present study, it was observed that TMEM14A induced the upregulation of LDHA both in OV cells and the murine tumor, which is in support of its role on promoting OV glycolytic process.

Wnt canonical (β-catenin-dependent) signaling pathway is the essential regulator of cell cycle and differentiation, while its deregulation and dysfunction can induce the initiation and progression of various types of human cancer, including OV (40,41). The aberrant cellular level and hyperactivity of β-catenin, the core factor for Wnt canonical pathway, initiates its translocation into nucleus where it binds and collaborates with various oncogene regulators for inducing oncogenesis in the cells (42,43). Our findings on that TMEM14A silencing could downregulate cellular β-catenin while its overexpression elevated β-catenin levels in OV cells illustrated the regulatory roles of TMEM14A in activating Wnt/β-catenin signals. In fact, they are in line with previous findings on that TMEM proteins may be critical for Wnt signaling transduction to further stabilize β-catenin in cells (44,45). At the other hand, Wnt/β-catenin pathway modulates multiple downstream protein effectors that directly regulate cell cycle and metabolic remodeling in OV, among which c-Myc proactively regulates carcinogenesis (46). Accordingly, it was identified that TMEM14A also influenced the cellular level of c-Myc in OV cells. Additionally, the simultaneous treatment of Wnt/β-catenin inhibitor counteracted the OV-promotive effect of TMEM14A overexpression, which further confirms the participation of TMEM14A in OV tumor cell programmed death and energy metabolism via the Wnt canonical pathway. Collectively, the comprehensive biological functions of TMEM14A in facilitating OV activities through regulating the Wnt/β-catenin pathway were revealed. Based on these findings, the present study contributed in seeking and developing OV diagnostic and prognostic biomarkers for clinical management as well as locating therapeutic targets for OV treatment. Overall, the short number of clinical samples that were used in present research limited the significance of our findings. Therefore, it will be of great value to further confirm the authenticity of our data in a larger number of clinical samples.

To summarize, the elevated expression of TMEM14A in OV tumorous tissues, its significant correlation with OV prognosis, as well as its pro-oncogenic roles in OV cellular activities, were demonstrated. These bio-functions include promoting cellular aerobic glycolysis and oxygen respiration, suppressing cell apoptosis *in vitro* and facilitating tumorigenicity in mice. Moreover, the underlying mechanism of these tumor-promotive effects may be dependent on the regulation of the Wnt/β-catenin signaling pathway by TMEM14A.

Acknowledgements

Not applicable.

Funding

The present study was supported by the Medical Innovation Project of Fujian Province (grant no. 2018-CX-44).

Availability of data and materials

The datasets generated and/or analyzed during the current study are not publicly available due to privacy or ethical restrictions but are available from the corresponding author on reasonable request.

Authors' contributions

JC, QZ, XW and XZ made substantial contributions to conception, design and acquisition of data. JZ, BZ and JJ made substantial contributions and analyzed the data. All authors contributed to the writing of the article and have read and approved the final manuscript. XW and XZ confirm the authenticity of all the raw data.

Ethics approval and consent to participate

The research protocol for patient studies was approved (approval no. 2019-017-02) by the ethics committee of People's Hospital Affiliated to Fujian University of traditional Chinese Medicine (Fuzhou, China) according to the Declaration of Helsinki. Written informed consents were provided from all patients enrolled in the present study. The animal trial was approved by the ethics committee of People's Hospital Affiliated to Fujian University of traditional Chinese Medicine and conducted following the guidelines of the institute.

Patient consent for publication

Not applicable.

Competing interests

The authors declare that they have no competing interests.

References

1. Bray F, Ferlay J, Soerjomataram I, Siegel RL, Torre LA and Jemal A: Global cancer statistics 2018: GLOBOCAN estimates of incidence and mortality worldwide for 36 cancers in 185 countries. CA Cancer J Clin 68: 394-424, 2018.
2. Reid BM, Permuth JB and Sellers TA: Epidemiology of ovarian cancer: A review. Cancer Biol Med 14: 9-32, 2017.
3. Momenimovahed Z, Tiznobaik A, Taheri S and Salehiniya H: Ovarian cancer in the world: Epidemiology and risk factors. Int J Womens Health 11: 287-299, 2019.
4. Jacobs IJ and Menon U: Progress and challenges in screening for early detection of ovarian cancer. Mol Cell Proteomics 3: 355-366, 2004.

5. Gajjar K, Ogden G, Mujahid MI and Razvi K: Symptoms and risk factors of ovarian cancer: A survey in primary care. ISRN Obstet Gynecol 2012: 754197, 2012.
6. Budiana ING, Angelina M and Pemayun TGA: Ovarian cancer: Pathogenesis and current recommendations for prophylactic surgery. J Turk Ger Gynecol Assoc 20: 47-54, 2019.
7. Han CY, Patten DA, Richardson RB, Harper ME and Tsang BK: Tumor metabolism regulating chemosensitivity in ovarian cancer. Genes Cancer 9: 155-175, 2018.
8. Kar R, Sen S, Singh A, Sharma H, Kumar S, Gupta SD and Singh N: Role of apoptotic regulators in human epithelial ovarian cancer. Cancer Biol Ther 6: 1101-1105, 2007.
9. Reed J, Hakam A, Nicosia SV and Coppola D: Significance of Fas receptor protein expression in epithelial ovarian cancer. Hum Pathol 36: 971-976, 2005.
10. Hay N: Reprogramming glucose metabolism in cancer: Can it be exploited for cancer therapy? Nat Rev Cancer 16: 635-649, 2016.
11. Bast RC Jr, Hennessy B and Mills GB: The biology of ovarian cancer: New opportunities for translation. Nat Rev Cancer 9: 415-428, 2009.
12. Li SS, Ma J and Wong AST: Chemoresistance in ovarian cancer: Exploiting cancer stem cell metabolism. J Gynecol Oncol 29: e32, 2018.
13. Marx S, Dal Maso T, Chen JW, Bury M, Wouters J, Michiels C and Calvé BL: Transmembrane (TMEM) protein family members: Poorly characterized even if essential for the metastatic process. Semin Cancer Biol 60: 96-106, 2020.
14. Schmit K and Michiels C: TMEM proteins in cancer: A review. Front Pharmacol 9: 1345, 2018.
15. Wang Y, Zhang Y, Herman JG, Linghu E and Guo M: Epigenetic silencing of TMEM176A promotes esophageal squamous cell cancer development. Oncotarget 8: 70035-70048, 2017.
16. Kayed H, Kleeff J, Ding J, Hammer J, Giese T, Zentgraf H, Büchler MW and Friess H: Expression analysis of MAC30 in human pancreatic cancer and tumors of the gastrointestinal tract. Histol Histopathol 19: 1021-1031, 2004.
17. Zhou X, Popescu NC, Klein G and Imreh S: The interferon-alpha responsive gene TMEM7 suppresses cell proliferation and is downregulated in human hepatocellular carcinoma. Cancer Genet Cytogenet 177: 6-15, 2007.
18. Doolan P, Clynes M, Kennedy S, Mehta JP, Germano S, Ehrhardt C, Crown J and O'Driscoll L: TMEM25, REPS2 and Meis 1: Favourable prognostic and predictive biomarkers for breast cancer. Tumour Biol 30: 200-209, 2009.
19. Flamant L, Roegiers E, Pierre M, Hayez A, Sterpin C, Backer OD, Arnould T, Poumay Y and Michiels C: TMEM45A is essential for hypoxia-induced chemoresistance in breast and liver cancer cells. BMC Cancer 12: 391, 2012.
20. Li B, Huang MZ, Wang XQ, Tao BB, Zhong J, Wang XH, Zhang WC and Li ST: TMEM140 is associated with the prognosis of glioma by promoting cell viability and invasion. J Hematol Oncol 8: 89, 2015.
21. Liu F, Cao QH, Lu DJ, Luo B, Lu XF, Luo RC and Wang XG: TMEM16A overexpression contributes to tumor invasion and poor prognosis of human gastric cancer through TGF-β signaling. Oncotarget 6: 11585-11599, 2015.
22. Qiao W, Han Y, Jin W, Tian M, Chen P, Min J, Hu H, Xu B, Zhu W, Xiong L and Lin Q: Overexpression and biological function of TMEM48 in non-small cell lung carcinoma. Tumour Biol 37: 2575-2586, 2016.
23. Hu R, Hu F, Xie X, Wang L, Li G, Qiao T, Wang M and Xiao H: TMEM45B, up-regulated in human lung cancer, enhances tumorigenicity of lung cancer cells. Tumour Biol 37: 12181-12191, 2016.
24. Cheng Z, Guo J, Chen L, Luo N, Yang W and Qu X: Overexpression of TMEM158 contributes to ovarian carcinogenesis. J Exp Clin Cancer Res 34: 75, 2015.
25. Yu X, Zhang X, Zhang Y, Jiang G, Mao X and Jin F: Cytosolic TMEM88 promotes triple-negative breast cancer by interacting with Dvl. Oncotarget 6: 25034-25045, 2015.
26. Hodo Y, Hashimoto S, Honda M, Yamashita T, Suzuki Y, Sugano S, Kaneko S and Matsushima K: Comprehensive gene expression analysis of 5'-end of mRNA identified novel intronic transcripts associated with hepatocellular carcinoma. Genomics 95: 217-223, 2010.
27. Smith JJ, Deane NG, Wu F, Merchant NB, Zhang B, Jiang A, Lu P, Johnson JC, Schmidt C, Bailey CE, *et al*: Experimentally derived metastasis gene expression profile predicts recurrence and death in patients with colon cancer. Gastroenterology 138: 958-968, 2010.
28. Zhang Q, Chen X, Zhang X, Zhan J and Chen J: Knockdown of TMEM14A expression by RNAi inhibits the proliferation and invasion of human ovarian cancer cells. Biosci Rep 36: e00298, 2016.
29. Livak KJ and Schmittgen TD: Analysis of relative gene expression data using real-time quantitative PCR and the 2(-Delta Delta C(T)) method. Methods 25: 402-408, 2001.
30. Qiu C, Duan Y, Wang B, Shi J, Wang P, Ye H, Dai L, Zhang J and Wang X: Serum Anti-PDLIM1 autoantibody as diagnostic marker in ovarian cancer. Front Immunol 12: 698312, 2021.
31. Wang N, Wang S, Li MY, Hu BG, Liu LP, Yang SL, Yang S, Gong Z, Lai PBS and Chen GG: Cancer stem cells in hepatocellular carcinoma: An overview and promising therapeutic strategies. Ther Adv Med Oncol 10: 1758835918816287, 2018.
32. Al-Alem LF, Baker AT, Pandya UM, Eisenhauer EL and Rueda BR: Understanding and targeting apoptotic pathways in ovarian cancer. Cancers (Basel) 11: 1631, 2019.
33. Cohen C, Lohmann CM, Cotsonis G, Lawson D and Santoianni R: Survivin expression in ovarian carcinoma: Correlation with apoptotic markers and prognosis. Mod Pathol 16: 574-583, 2003.
34. Tennant DA, Duran RV and Gottlieb E: Targeting metabolic transformation for cancer therapy. Nat Rev Cancer 10: 267-277, 2010.
35. Dar S, Chhina J, Mert I, Chitale D, Buekers T, Kaur H, Giri S, Munkarah A and Rattan R: Bioenergetic adaptations in chemoresistant ovarian cancer cells. Sci Rep 7: 8760, 2017.
36. Mookerjee SA, Goncalves RLS, Gerencser AA, Nicholls DG and Brand MD: The contributions of respiration and glycolysis to extracellular acid production. Biochim Biophys Acta 1847: 171-181, 2015.
37. Miao P, Sheng S, Sun X, Liu J and Huang G: Lactate dehydrogenase A in cancer: A promising target for diagnosis and therapy. IUBMB Life 65: 904-910, 2013.
38. Schneider D, Halperin R, Langer R, Bukovsky I and Herman A: Peritoneal fluid lactate dehydrogenase in ovarian cancer. Gynecol Oncol 66: 399-404, 1997.
39. Xiang J, Zhou L, Zhuang Y, Zhang J, Sun Y, Li S, Zhang Z, Zhang G and He Y: Lactate dehydrogenase is correlated with clinical stage and grade and is downregulated by siSATauB1 in ovarian cancer. Oncol Rep 40: 2788-2797, 2018.
40. Nguyen VHL, Hough R, Bernaudo S and Peng C: Wnt/β-catenin signalling in ovarian cancer: Insights into its hyperactivation and function in tumorigenesis. J Ovarian Res 12: 122, 2019.
41. Sheikh A, Niazi AK, Ahmed MZ, Iqbal B, Anwer SM and Khan HH: The role of Wnt signaling pathway in carcinogenesis and implications for anticancer therapeutics. Hered Cancer Clin Pract 12: 13, 2014.
42. Krishnamurthy N and Kurzrock R: Targeting the Wnt/beta-catenin pathway in cancer: Update on effectors and inhibitors. Cancer Treat Rev 62: 50-60, 2018.
43. Shang S, Hua F and Hu ZW: The regulation of β-catenin activity and function in cancer: Therapeutic opportunities. Oncotarget 8: 33972-33989, 2017.
44. Cong F, Schweizer L and Varmus H: Wnt signals across the plasma membrane to activate the beta-catenin pathway by forming oligomers containing its receptors, Frizzled and LRP. Development 131: 5103-5115, 2004.
45. MacDonald BT, Tamai K and He X: Wnt/beta-catenin signaling: Components, mechanisms, and diseases. Dev Cell 17: 9-26, 2009.
46. Bodnar L, Stanczak A, Cierniak S, Smoter M, Cichowicz M, Kozlowski W, Szczylik C, Wieczorek M and Lamparska-Przybysz M: Wnt/β-catenin pathway as a potential prognostic and predictive marker in patients with advanced ovarian cancer. J Ovarian Res 7: 16, 2014.